High Temp. Mater. Proc. 2013; 32(2): 107–111 DOI 10.1515/htmp-2012-0117

Structural and Mechanical Properties of Nanostructured TiAlCrN Thin Films Deposited by Cathodic Arc Deposition

N. Vattanaprateep,[1] **N. Panich,**[2] **S. Surinphong,**[3] **S. Tungasmita**[2,4] **and P. Wangyao**[5,*]

[1] Nanoscience and Technology, Graduate School, Chulalongkorn University, Bangkok, Thailand

[2] Center of Innovative Nanotechnology, Chulalongkorn University, Bangkok, Thailand

[3] NanoShield Company Limited, Samutprakarn, Thailand

[4] Department of Physics, Faculty of Science, Chulalongkorn University, Bangkok, Thailand

[5] Metallurgical Engineering Department, Engineering Faculty, Chulalongkorn University, Bangkok, Thailand

Abstract. This work has aims to study and develop the novel nanostructural quaternary thin film material for cutting tools and other applications with both high hardness value and good thermal stability at high temperature. The quaternary compound of TiAlCrN superhard coating material was deposited on tungsten carbide (WC-Co) substrates using cathodic arc deposition techniques at the deposition temperature of 623 K. The structures of the coatings were fundamentally examined by X-ray diffraction (XRD), scanning electron microscopy (SEM), energy dispersive spectrometer (EDS), and atomic force microscopy (AFM). The coating hardness and elastic modulus tests were performed and investigated by nanoindentation testing method. The maximum hardness and elastic modulus values as measured by nanoindentation tests are at 53 GPa and 887 GPa, respectively. Scratch tests were performed on thin films deposited in various conditions. The critical loads to the coating failure of the resultant coatings are above 75 N.

Keywords. TiAlCrN coatings, cathodic arc deposition, nanoindentation, XRD, SEM, AFM, hardness.

1 Introduction

At present, metallic nitride compound materials can be deposited on various substrates for many engineering applications in order to extend the lifespan and increase the hardness, adhesion, wear resistance, thermal stability,oxidation resistance and corrosive properties of those industrial tools. The structural and mechanical properties of hard coatings materials, based on titanium–aluminium nitride of transition metals, can be also enhanced by adding with other elements such as Al, Si, Cr, V, Y, B, Hf, Nb, etc. Each property above depends on material specifications and the coating processes [1].

Generally, nanostructured materials can be defined as materials with microstructures on length scales from several nanometers to 100 nm in at least one dimension. Using this working definition, nanostructured materials can be in the forms of cluster, thin film, coating and bulk materials. In term for nanostructure materials, nanocomposite materials for coatings show that the hardness can be significantly exceeded a rule of mixture. General speaking the industrial hard coating can be divided into 3 classes i.e. hard materials with the hardness less than 40 GPa, superhard materials with the hardness in the between 40–80 GPa and Ultrahard materials with the hardness above 80 GPa, in which each one relies on coating designs and applications. In terms of chemical composition, nanostructured materials can include nanostructured pure metal, alloys and nanocomposites [2–5].

At present, many technologies have shifted to ever smaller scales. Characterization of the mechanical properties of materials has then become more difficult and complicated. Among the techniques to measure the mechanical properties of nanostructured thin films or coatings, nanoindentation and microscratch testing techniques have been commonly used to evaluate thin film mechanical properties such as hardness, elastic modulus, scratch resistance, wear and coefficient of friction. Other main reason for the popularity of nanoindentation tests is that the mechanical properties can be measured without removing the film from its substrate, which contrasts to carry out by other types of testing such as conventional hardness test.

For Ti-Al-Cr-N coating material, the role of chemical compositions of thin film study was found that as the Cr content increased, it can enhance mechanical properties such as hardness and elastic modulus [6, 7]. Usually, the results from nanoindentation tests of TiAlCrN show the hardness and elastic modulus values in the range of 38.4 GPa to 500 GPa, respectively [8]. The researchers explained that with increasing percentage of Cr, the preferred orientation

* **Corresponding author:** P. Wangyao, Metallurgical Engineering Department, Engineering Faculty, Chulalongkorn University, Bangkok, Thailand; E-mail: panyawat@hotmail.com.

Received: March 3, 2011. Accepted: April 1, 2011.

shifted from (200) planes to (111) planes which possess the highest hardness [9].

Attempts have been made to investigate the microstructures and mechanical properties (hardness and elastic modulus) of TiAlCrN thin films prepared by cathodic arc plasma evaporation. The effect of adding Ti and Al into the material resulted in microstructural changes leading to an improvement in mechanical properties of the thin films.

2 Materials and Experimental Procedures

In this study, TiAlCrN thin film materials of different elemental compositions were synthesized in an industrial PVD cathodic arc deposition system (NanoShield Ltd. NS-1), which equipped with 2 NanoShield Metal Plasma sources and 3 Advanced Steered Arc sources specially made for NanoShield Ltd. by D. V. Efremov Scientific Research Institute, Russia. A Chromium target and two TiAl targets with different Ti:Al atomic ratio were used in the growth processes, as shown in Figure 1. The target configurations are shown in Table 1. Carbide coupons (WC with Co binder) substrates were polished and ultrasonically cleaned in trichloroethylene solvent then they were blown-drier before placing into the chamber. After evacuation until pressure drop down to 5.0×10^{-3} Pa at the substrate temperature up to 623 K. The substrates were cleaned and sputtered by the Ar glow discharge. Then the samples were cleaned further by Titanium plasma from NanoShield Metal Plasma sources. And the metallic glue layers were done with the same Metal Plasma Sources for better adhesion. Depositions of TiAlCrN were carried out under Nitrogen atmosphere with working pressure of 1.5 Pa. The substrates were applied a bias voltage at −100 V during deposition at 623 K. The calculated deposition rate was about 24–25 nm/min with the thicknesses in the range of about 3–5 μm for resultant film characterizations.

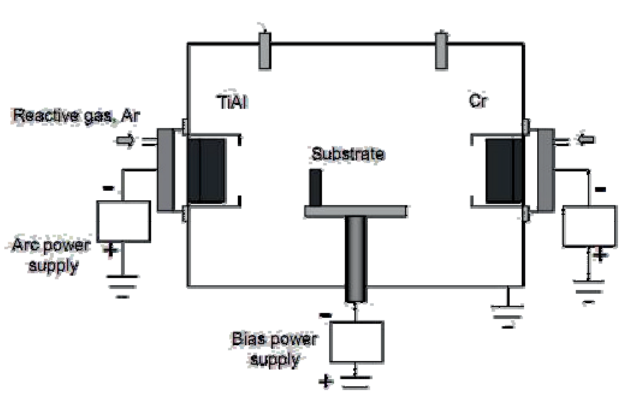

Figure 1. Schematic diagram cathodic arc evaporation (CAE).

Batch	Target 1	Target 2	Target 3	Target 4
1	$Ti_{33}Al_{67}$	$Ti_{33}Al_{67}$	Cr	–
2	$Ti_{50}Al_{50}$	$Ti_{50}Al_{50}$	Cr	–
3	$Ti_{50}Al_{50}$	Ti	Cr	–
4	$Ti_{33}Al_{67}$	$Ti_{33}Al_{67}$	Cr	Al

Table 1. Target configuration for TiAlCrN coatings.

Surface morphology of the films had been observed by scanning electron microscope, SEM (JSM-5800LV, JEOL). The elemental compositions of films were examined by using Energy dispersive spectroscopy (EDS). X-ray diffractometer was used for the crystal structure analysis and study the preferred orientations of the coating layers. The root-mean-square (RMS) roughnesses of the films were measured by Atomic force microscopy, AFM (Innova, Model: 840-012-711). The mechanical properties of the layers were characterized by NHT Nanoindentor (CSM-instruments) with the indentation depth at 10% of the film thickness under a constant loading and unloading of 10 mN/60 s. The coating adhesion test was evaluated by a scratch tester (Revetest, CSM).

3 Results and Discussion

3.1 Structural and Elemental Compositions Characterizations

This research had fabricated the TiAlCrN thin films with different elemental compositions from different Ti:Al ratio and arc source. Figure 2 shows the morphology of deposited coatings. It can be seen that the surface morphologies of the TiAlCrN film showed some macro particles, which had occurred from the targets of both materials in CAE process by dimensional size 1–10 μm. The investigation in macro particle have high percentage of N and percentage of Cr more in 1^{st}, 2^{nd} and 3^{rd} batches. Therefore, it is supposed to be CrN phase, which is the same as the proposed of Munz et al. [10]. 4^{th} batch shows the appearance of macro particles and has percentages of N, Al and Cr. Therefore, they probably are AlN and CrN phases. The elemental compositions of films were examined by using EDS. The compositions of as-deposited films are shown in the Table 2 (in atomic percent).

In this work, it had been also studied4 batches for difference of element compositions in the films. In 1^{st} and 2^{nd} batches comparing TiAl ratio between $Ti_{33}Al_{67}$ and $Ti_{50}Al_{50}$ respectively, it was found that both percentages of N are alike (1^{st} = 53.31%at. and 2^{nd} = 53.18%at.). In the 1^{st} batch, $Ti_{0.23}Al_{0.36}Cr_{0.4}N$, consists of high Cr content and in the 2^{nd} batch, $Ti_{0.36}Al_{0.27}Cr_{0.37}N$, %Ti was increased but %Al and %Cr were decreased. In 3^{rd} batch, $Ti_{0.46}Al_{0.20}Cr_{0.34}N$ (which was modified by adding one

Batch	**Ti (at %.)**	**Al (at %)**	**Cr (at %)**	**N (at %)**	**Elemental composition**	**Root-mean-square (RMS) Roughness (nm)**
1	10.65	16.63	19.41	53.31	$Ti_{0.23}Al_{0.36}Cr_{0.4}N$	76
2	16.5	12.97	17.35	53.18	$Ti_{0.36}Al_{0.27}Cr_{0.37}N$	66
3	22.84	10.08	16.74	50.34	$Ti_{0.46}Al_{0.20}Cr_{0.34}N$	29
4	9.30	28.06	15.85	46.79	$Ti_{0.17}Al_{0.53}Cr_{0.30}N$	97

Table 2. Elemental compositions of TiAlCrN thin film.

Elemental composition	**Hardness [GPa]**	**Elastic modulus [GPa]**	**H /E**
$Ti_{0.23}Al_{0.36}Cr_{0.40}N$	44	615	0.0715
$Ti_{0.36}Al_{0.27}Cr_{0.37}N$	47	667	0.0705
$Ti_{0.46}Al_{0.20}Cr_{0.34}N$	53	887	0.0597
$Ti_{0.17}Al_{0.53}Cr_{0.30}N$	42	454	0.0925

Table 3. Mechanical properties of TiAlCrN thin film.

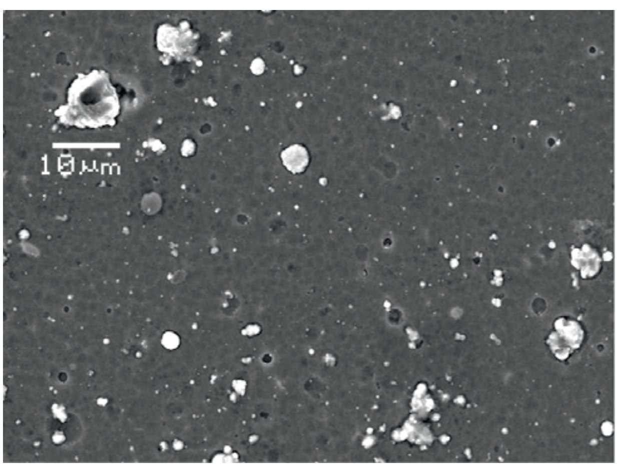

Figure 2. SEM image of morphology of deposited coating.

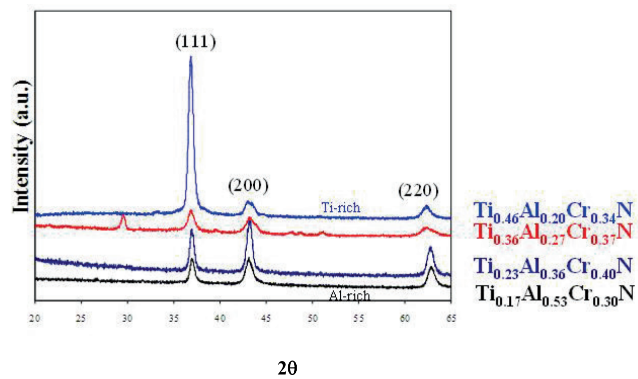

Figure 3. XRD patterns of TiAlCrN coating.

pure Ti), %Ti reached to 22.84 %wt. In the 4th batch required as designed with high Al composition by using $Ti_{33}Al_{67}$ target and added Al source, $Ti_{0.17}Al_{0.53}Cr_{0.30}N$, it was found the lowest %N of 46.79% with Al up to 28.06%.

The surface roughness, Root-mean-square (RMS) method, was measured by Atomic force microscopy (AFM). The results are shown in the Table 2. $Ti_{0.46}Al_{0.20}Cr_{0.34}N$ (Ti-rich) has minimum value of RMS at 29 nm. Thus, $Ti_{0.46}Al_{0.20}Cr_{0.34}N$ is the smoothest surface due to high percentage of Ti in chemical composition when comparing with $Ti_{0.17}Al_{0.53}Cr_{0.30}N$ (highest Al, lowest Ti and Cr). According to Table 2, $Ti_{0.17}Al_{0.53}Cr_{0.30}N$ shows the highest RMS surface roughness (97 nm), which RMS values follow %Al. The result corresponding to %Al increases with an increase in RMS, conversely, the results show %Ti increases with a decrease in RMS.

Figure 3 shows the X-Ray Diffraction results. All of TiAlCrN films were found in mixed orientation of (111), (200) and (220) crystal planes respectively, which is similar to literatures [4–6]. It was found that $Ti_{0.46}Al_{0.20}Cr_{0.34}N$ coating with a high Ti-content shows the preferred orientation of (111), which matches the peak for NaCl-type structure and most stable and has the highest packing atoms. Other peaks, (111) and (200), are nearby $Ti_{0.23}Al_{0.36}Cr_{0.4}N$ (1st batch) preferred orientation (200) as it is in a good agreement with the observation of [11]. $Ti_{0.36}Al_{0.27}Cr_{0.37}N$ (2nd batch) changed peak from (200) to (111). $Ti_{0.46}Al_{0.20}Cr_{0.34}N$ (3rd batch) shows clearly preferred orientation (111). $Ti_{0.17}Al_{0.53}Cr_{0.30}N$ (4th batch) was found that exhibits in the same way (111) and (200). There are some competitive growth between (200) and (111) due to stress in the crystal structure of the alloy films. In general, XRD peak broadening is believed to originate from the diminution of grain size or the residual stress in-

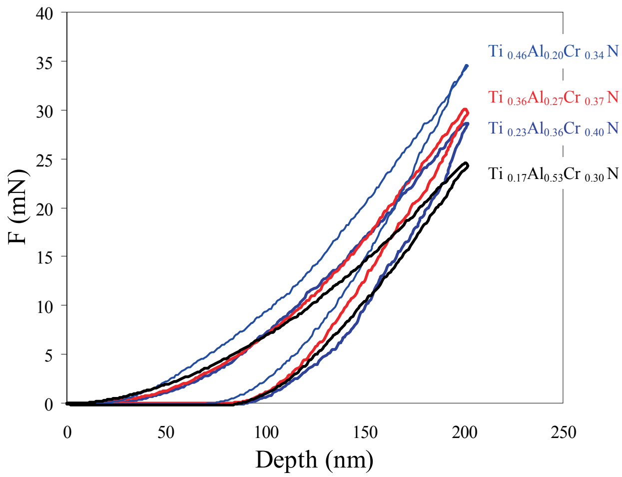

Figure 4. Load-displacement curves of TiAlCrN.

duced in the crystal lattice [3, 4]. The XRD peak shape of TiAlCrN films was broadened with an increase of Ti contents and decrease of Al-contents. The beyond, XRD result showed the observed peaks were moved forward (a bit) shifted (111) in comparison with other peaks.

3.2 Mechanical properties

Figure 4 shows typical nanoindentation load-unload curves recorded for the fourth coating systems. The average hardness and reduced modulus derived from 6 measurements for each coating are summarized in Table 3. It can be seen that the $Ti_{0.46}Al_{0.20}Cr_{0.34}N$ resulting in higher hardness and elastic modulus evidently presenting the load-unload curves shown in Figure 4, which the $Ti_{0.46}Al_{0.20}Cr_{0.34}N$ coating with a high titanium exhibits greater resistance to indentation and larger elastic recovery during the unloading stage. Table 3 shows mechanical properties of thin films tested by nanoindentation by comparing results between 1st and 2nd batches. The different TiAl ratio was found that at TiAl ratio 50 : 50 ($Ti_{0.36}Al_{0.27}Cr_{0.37}N$) provides better results than those of $Ti_{33}Al_{67}$ ($Ti_{0.23}Al_{0.36}Cr_{0.4}N$). It can be taken into account that different elemental composition, which has high Ti content provides harder phase and low Al content provides softer phase [10]. We found that preferred orientation exhibit in $Ti_{0.36}Al_{0.27}Cr_{0.37}N$ when increase %Ti. The decrease %Al was found changing from (200) to (111), which similarly to [8–10].

In next batch we have modified experiment by adding Ti source to increase more Ti concentration. The results from EDS showed that at the highest Ti and the lowest %Al, $Ti_{0.46}Al_{0.20}Cr_{0.34}N$ reached up to maximum hardness and modulus, 53 GPa and 887 GPa, respectively. Crystalline formation had explained that preferred orientation (111) is very sharp when comparing with that of other smaller peaks, which explained by means of superior of hardness. The study of toughness by study H/E ratio proved that the lowest 0.0597 showed higher toughness than another, which is similar to work of Santana et al. [8].

In final batch, the experiment was designed at high Al, by adding Al source. It was found that $Ti_{0.17}Al_{0.53}Cr_{0.30}N$ had the lowest hardness and elastic modulus of 42 GPa and 454 GPa, respectively with the preferred orientation of both (111) and (200). In the same study of H/E ratio with highest 0.0925 value, it shows a low toughness properties.

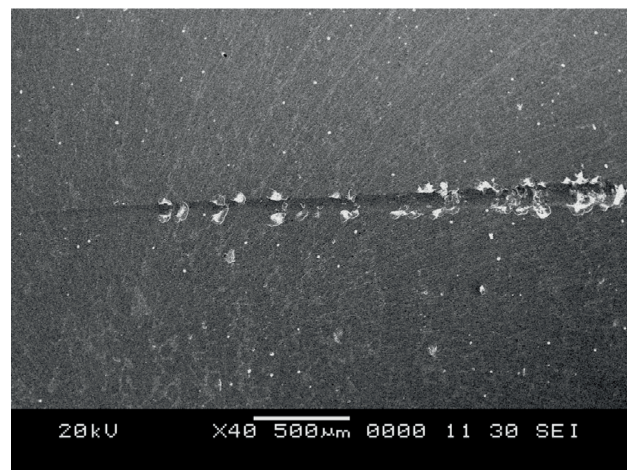

Figure 5. SEM image of scratch track of TiAlCrN film.

Figure 5 shows the SEM image of typical scratch tracks of TiAlCrN. Scratch tests on these films exhibited critical load higher than 75 N, whereas films deposited high Al with low Ti ($Ti_{0.17}Al_{0.53}Cr_{0.30}N$) showed very low critical load. In order to identify the failure modes of the coatings, the SEM images were further examined, it was found that compressive spallation occurs in most of the coating typically due to a very high hardness.

4 Conclusion

1. Ti-Al-Cr-N coating system can be fabricated on WC-Co deposited by the cathodic arc techniques. The results of the microstructures and mechanical properties were summarized in this paper clearly indicating especially hardness and modulus.

2. Based on the results, chemical composition in the films can be controlled by changing TiAl ratio in the target. It can be concluded that Ti and Al contents play a major role in microstructure and hardness of Ti-Al-Cr-N coatings.

3. The increase in Ti content and reduce in Al content of Ti-Al-Cr-N provide a rise of hardness values, which were increased from 42 GPa with the 9.30% of Ti to 53 GPa with the 22.84% of Ti. As well as, modulus

values were increases from 454 GPa to 887 GPa., due to preferred orientation changing from (200) to (111) crystal hard phase with lowest RSM roughness.

4. As the Ti content increases with low percentage of Al, $Ti_{0.46}Al_{0.20}Cr_{0.34}N$ is a film with great mechanical properties, hard materials and good ductility.

References

[1] J. Musil, Surface & Coatings Technology, **125** (2000), 322–330.

[2] A. Raveh, I. Zukerman, R. Shneck, R. Avni and I. Fried, Surface & Coatings Technology, **201** (2007), 6136–6142.

[3] S. Veprek, M. G. J. Veprek-Heijman, P. Karvankova and J. Prochazka, Thin Solid Films, **476** (2005), 1–29.

[4] S. Vepfek and S. Reiprich, Thin Solid Films, **268** (1995), 64–71.

[5] A. Niederhofer, T. Bolom, P. Nesladek, K. Moto, C. Eggs, D. S. Patil1 and S. Veprek, Surface & Coatings Technology, **146–147** (2001), 183–188.

[6] A. I. Kovalev, D. L. Wainstein, A. Y. Rashkovskiy, G. S. Fox-Rabinovich, K. Yamamoto, S. Veldhuis, M. Aguirr and D. B. Beake, Vacuum, **84** (2010), 184–187.

[7] G. S. Fox-Rabinovich, K. Yamomota, S. C. Veldhuis, A. I. Kovalev and G. K. Dosbaeva, *Surface & Coatings Technology*, **200** (2005), 1804–1813.

[8] A. E. Santana, A. Karimi, V. H. Derflinger and A. Schutze, Surface & Coatings Technology, **177–178** (2004), 334–340.

[9] K. Yamamoto, T. Sato, K. Takahara and K. Hanaguri, Surface & Coatings Technology, **174–175** (2003), 620–626.

[10] W. D. Munz, L. A. Donohue and P. Eh. Hovsepian, Surface & Coatings Technology, **125** (2000), 269–277.

[11] J. L. Endrino and V. Derflinger, Surface &Coatings Technology, **200** (2005), 988–992.